BIOCHEMISTRY
including biophysical chemistry & molecular biology
Article

Biochemistry **2009,** *48,* 4895–4904 4895
DOI: 10.1021/bi802235w

Dynamic Conformational Responses of a Human Cannabinoid Receptor-1 Helix Domain to Its Membrane Environment†

Elvis K. Tiburu,[‡,||] Stefano V. Gulla,[§,||] Mark Tiburu,[‡] David R. Janero,[‡] David E. Budil,*[,§] and Alexandros Makriyannis*[,‡]

[‡]*Center for Drug Discovery and* [§]*Department of Chemistry and Chemical Biology, Northeastern University, Boston, Massachusetts 02115-5000* [||]*E.K.T.and S.V.G. contributed equally to this work*

Received December 8, 2008; Revised Manuscript Received March 25, 2009

ABSTRACT: The influence of membrane environment on human cannabinoid 1 (hCB_1) receptor transmembrane helix (TMH) conformational dynamics was investigated by solid-state NMR and site-directed spin labeling/EPR with a synthetic peptide, hCB_1(T377-E416), corresponding to the receptor's C-terminal component, i.e., TMH7 and its intracellular α-helical extension (H8) (TMH7/H8). Solid-state NMR experiments with mechanically aligned hCB_1(T377-E416) specifically ^2H- or ^{15}N-labeled at Ala380 and reconstituted in membrane-mimetic dimyristoylphosphocholine (DMPC) or 1-palmitoyl-2-oleoyl-*sn*-glycerophosphocholine (POPC) bilayers demonstrate that the conformation of the TMH7/H8 peptide is more heterogeneous in the thinner DMPC bilayer than in the thicker POPC bilayer. As revealed by EPR studies on hCB_1(T377-E416) spin-labeled at Cys382 and reconstituted into the phospholipid bilayers, the spin label partitions actively between hydrophobic and hydrophilic environments. In the DMPC bilayer, the hydrophobic component dominates, regardless of temperature. Mobility parameters (ΔH_0^{-1}) are 0.3 and 0.73 G for the peptide in the DMPC or POPC bilayer environment, respectively. Interspin distances of doubly labeled hCB_1(T377-E416) peptide reconstituted into a TFE/H_2O mixture or a POPC or DMPC bilayer were estimated to be 10.6 ± 0.5, 16.8 ± 1, and 11.6 ± 0.8 Å, respectively. The extent of coupling (≥50%) between spin labels located at i and $i + 4$ in a TFE/H_2O mixture or a POPC bilayer is indicative of an α-helical TMH conformation, whereas the much lower coupling (14%) when the peptide is in a DMPC bilayer suggests a high degree of peptide conformational heterogeneity. These data demonstrate that hCB_1(T377-E416) backbone dynamics as well as spin-label rotameric freedom are sensitive to and altered by the peptide's phospholipid bilayer environment, which exerts a dynamic influence on the conformation of a TMH critical to signal transmission by the hCB_1 receptor.

Signal-transducing G protein-coupled receptors (GPCRs)[1] are proteins that share as a common defining structural signature an intracellular carboxyl terminus, seven hydrophobic transmembrane helices (TMHs) connected by intra- and extracellular loops, and an extracellular amino terminus (*1*). Agonist binding is believed to induce ligand-specific GPCR structural changes that allow the receptor to assume, likely through a continuum of intermediate conformations, a functionally active state (*2*−*4*). GPCR conformation, activity, and intracellular trafficking may also be modulated by local membrane properties (e.g., tension, fluidity, lateral pressure) in the absence of agonist binding (*5*, *6*). Such ligand-independent GPCR responses imply that the membrane phospholipid bilayer itself may modulate GPCR signal transmission, congruent with the general importance of lipid−protein interactions to membrane protein function (*7*). Regardless of the agonist- or membrane-related influences involved, however, the molecular mechanisms responsible for GPCR conformational transition, the natures of the resulting receptor structural states, and the relationships between GPCR conformation and the triggering of distinct effector circuitry are largely ill-defined (*1*, *2*). Given that GPCRs represent prime pharmaceutical targets and some 40% of known drugs exert their therapeutic action by interacting with them (*1*), GPCR conformational plasticity has great biomedical and translational relevance.

Among the GPCRs so far identified, the two main cannabinoid (CB) receptor subtypes, designated CB_1 and CB_2, have

†This study was supported by National Institutes of Health/National Institute on Drug Abuse Grants DA009158-10S2 (E.K.T.) and DA3801 (A.M.) and National Science Foundation Instrumentation Grant CHE-0466616 (D.E.B.).

*Corresponding authors. A.M.: phone, (617) 373-4200; fax, (617) 373-7493; e-mail, a.makriyannis@neu.edu. D.E.B.: phone, (617) 373-2369; fax, (617) 373-8795; e-mail, d.budil@neu.edu.

[1]Abbreviations: A_{iso}, isotropic hyperfine splitting; CB, cannabinoid; CB_2, cannabinoid 2; DMPC, dimyristoylphosphocholine; EPR, electron paramagnetic resonance; Fmoc, 9*H*-fluoren-9-ylmethoxycarbonyl; GPCR, G protein-coupled receptor; H, helix; ΔH_0^{-1}, mobility parameter; hCB_1, human cannabinoid 1; HEPES, *N*-(2-hydroxyethyl)piperazine-*N*′-2-ethanesulfonic acid; NMR, nuclear magnetic resonance; POPC, 1-palmitoyl-2-oleoyl-*sn*-glycerophosphocholine; $R_{||}$, parallel rotational correlation time; $R_{\perp}$, perpendicular rotational correlation time; SDSL, site-directed spin labeling; TFE, 2,2,2-trifluoroethanol; TMH, transmembrane helix.

 Published on Web 05/04/2009

gained intense interest as potential therapeutic targets (*8*). The CB_1 receptor is expressed principally in brain regions that influence mood and reward-related behaviors. The CB_2 receptor is largely peripheral, found mainly in immune and white blood cells (*9*). CB_1 and CB_2 receptors are activated by a variety of exogenous natural cannabinoids (e.g., the plant cannabinoid Δ^9-tetrahydrocannabinol), endogenous cannabinoid agonists (endocannabinoids) (e.g., anandamide and 2-arachidonoylglycerol), and synthetic cannabimimetics, the latter often designed with high selectivity for one particular CB-receptor subtype (*8*, *10*, *11*). Depending somewhat upon the activating ligand, these CB receptors primarily couple to inhibitory G proteins ($G_{i/o}$) during signal transduction (*9*). The psychotrophic effects of Δ^9-tetrahydrocannabinol are largely mediated through CB_1 receptors in the central nervous system (*12*), and the first-in-class ethical pharmaceutical designed to modulate endocannabinoid-system activity, rimonabant, is a CB_1-receptor antagonist (*13*). Consequently, the CB_1 receptor has been targeted by designer small-molecule ligands to treat such pressing medical problems as overweight/obesity and associated cardiometabolic risk, metabolic syndrome, drug addiction, and substance abuse (*8*, *13*, *14*).

In order to exploit the CB_1 receptor safely and effectively for therapeutic purposes, an operational understanding of the determinants of CB_1-receptor conformation is essential. Although rhodopsin's X-ray crystal structure has enabled homology modeling of CB receptors in lieu of their crystal structures being solved (*11*, *15*−*19*), the inherent extrapolations involved (*16*, *20*) and the many distinguishing features of CB receptors, including relatively long N- and C-termini implicated in their activity and stability (*16*−*18*), mandate direct experimental analysis of CB-receptor structure and dynamics. The CB_1-receptor C-terminal region appears to be particularly critical to the conformational transitions leading to receptor activation and the docking of specific G-protein subtypes (*15*, *19*). Here, we describe the conformation and dynamics of a synthetic peptide [hCB_1(T377-E416)][2] that corresponds, by rhodopsin homology modeling, to the hCB_1 receptor's C-terminal component, i.e., the hCB_1 receptor segment consisting of TMH7 (T377-L399) and its intracellular α-helical extension (H8) (L404-E416) (*17*−*21*). TMH7 includes Ser383, a ligand-interaction site that plays a crucial role in hCB_1 receptor agonist recognition and activation (*17*). We have reconstituted hCB_1(T377-E416) into mechanically oriented (*22*, *23*) dimyristoylphosphocholine (DMPC) and 1-palmitoyl-2-oleoyl-*sn*-glycerophosphocholine (POPC) phospholipid bilayer environments prior to solid-state nuclear magnetic resonance (NMR) and site-directed spin labeling (SDSL)/electron paramagnetic resonance (EPR) spectroscopic analyses. Whereas solid-state NMR spectroscopy has been applied to investigate CB-receptor TMH orientation (*22*), to the authors' knowledge, SDSL/EPR has not heretofore been used to probe CB-receptor structure. Using these experimental approaches, we define in this report specific conformational aspects of a CB_1-receptor TMH7/H8 peptide sensitive to and dynamically modulated by its membrane phospholipid matrix.

EXPERIMENTAL PROCEDURES

Materials. POPC and DMPC in chloroform (Avanti Polar Lipids, Alabaster, AL) were stored at −20 °C prior to use. 2,2,2-Trifluoroethanol (TFE), *N*-(2-hydroxyethyl)piperazine-*N*′-2-ethanesulfonic acid (HEPES), EDTA, deuterium-depleted water, and most other chemicals were purchased from Sigma-Aldrich (St. Louis, MO). The spin label, 3-(iodomethyl)-2,2,5,5-tetramethyl-2,5-dihydropyrrole-1-oxyl, was from Toronto Research Chemicals (Toronto, Ontario, Canada). CD_3- and ^{15}N-Ala were purchased from Cambridge Isotope Laboratories (Andover, MA).

Peptide Synthesis and Purification. The TMH7/H8 peptide 40-mer, hCB_1(T377-E416), was produced by standard methodology using an Applied Biosystems synthesizer equipped for 9*H*-fluoren-9-ylmethoxycarbonyl (Fmoc) chemistry (GenScript Corp., Piscataway, NJ). A CD_3- or ^{15}N-Ala was incorporated at position 380 during peptide synthesis. All amino acids were single coupled with a total of 9.5 min for the coupling and monitoring module. The crude peptide was isolated to 95% purity by LC. MALDI-TOF mass spectrometry using an α-cyano-4-hydroxycinnamic acid calibration matrix revealed a peptide m/z of 4583.36.

Peptide Spin Labeling. Samples were prepared for SDSL by resuspending lyophilized hCB_1(T377-E416) peptide (95% purity) in a solution of 4 M guanidine hydrochloride and adding an appropriate amount of 0.1 M stock solution of 3-(iodomethyl)-2,2,5,5-tetramethyl-2,5-dihydropyrrole-1-oxyl to achieve a final molar ratio of 1:3 peptide to spin label. The mixture was incubated overnight at 4 °C. Unreacted spin label was removed by dialysis with a 500 Da cutoff membrane prior to reverse-phase LC peptide purification to 95%. Mass spectrometry confirmed the singly and doubly spin-labeled hCB_1(T377-E416) to have m/z = 4636 and 4789, respectively. Nitroxide activity was verified by EPR. The labeling efficiency was estimated by LC-MS to be ∼90%. All experiments were conducted from the same stock of labeled peptide.

Sample Preparation for NMR and EPR. Samples of hCB_1(T377-E416) incorporated in DMPC and POPC bilayers were prepared according to literature protocol, as slightly modified (*22*−*25*). Appropriate amounts of hCB_1(T377-E416) peptide dissolved in minimal TFE and either DMPC or POPC dissolved in chloroform (20 mg/mL) were mixed to give a 1:100 peptide-to-lipid molar ratio (*26*). Solvent was removed under a nitrogen stream at ambient temperature, and the dried samples were held overnight in a vacuum desiccator. For NMR, the ^{2}H/^{15}N-labeled powder sample was then packed into a 4 mm ZrO_2 rotor. A hydrated sample was prepared by incubating the rotor containing the powder sample in a sealed chamber with saturated ammonium monophosphate (relative humidity ∼93%) for 6−12 h at 45 °C.

A mechanically aligned sample was prepared by mixing hCB_1(T377-E416) with either DMPC or POPC to achieve a 1:100 peptide-to-lipid molar ratio (as above) in a pear-shaped flask. Nitrogen gas was passed through the resulting mixture until the chloroform volume was reduced by two-thirds. The sample was spread onto 25 glass plates (8.5 mm × 14 mm), which were dried overnight in a desiccator (*27*). Deuterium-depleted water was introduced onto each dried peptide−lipid mixture, and the glass plates were stacked on top of one other. The stack was then placed into an ammonium monophosphate chamber (relative humidity ∼93%) at 42 °C until the sample became transparent, indicating complete incorporation of hCB_1(T377-E416) peptide into either phospholipid bilayer.

Solid-State NMR Spectroscopy. All NMR spectra were routinely collected at 35 °C (308 K). Quadrupolar echo pulse

[2]The Ballesteros and Weinstein universal numbering scheme for class A GPCRs is used herein (*20*). Amino acid positions designated are those in the full-length, wild-type human CB_1 receptor.

sequence (*28*) was used for the ^{2}H NMR studies with quadrature detection capabilities and complete phase cycling of the pulse pairs. A 3.0 μs 90° pulse, 100 kHz sweep width, 400 ms recycle delay, and 30 μs interpulse delay were used to accumulate 200000 transients. Prior to Fourier transformation, an exponential multiplication of 200 Hz line broadening was performed on the spectra. ^{15}N NMR spectra were collected utilizing a standard cross-polarization pulse sequence with ^{1}H decoupling (*29*). For the ^{15}N-labeled aligned samples, the following pulse sequence parameters were used: 4.7 μs ^{1}H 90°, 500 ppm sweep width, 1.5 ms contact time, and 4 s recycle delay with ^{1}H decoupling (*30*−*32*). The ^{15}N NMR spectra were referenced to an external standard of $(^{15}NH_4)_2SO_4$ (27 ppm). For ^{2}H- and ^{15}N-labeled, mechanically aligned samples, a double resonance flat coil probe was used, operating at the required temperature in an Ultrashield Plus AVANCE 700 MHz spectrometer (Bruker Daltonics, Billerica, MA).

EPR Spectroscopy. EPR spectroscopy was carried out with a Bruker EMX instrument equipped with a high-sensitivity cylindrical cavity and a variable-temperature module. For aqueous samples at 35−80 °C (308−353 K), spectra were acquired at a microwave frequency of 9.37 GHz, 2.0 mW microwave power, and 0.5 G 100 kHz field modulation amplitude. Rigid limit spectra were acquired under the same conditions, but at −123 °C (150 K), 0.2 mW microwave power, and 1.0 G 100 kHz field modulation amplitude.

RESULTS

Solid-State NMR Studies of hCB$_1$(T377-E416) in Phospholipid Membrane Bilayers. Homology modeling of the CB$_1$ receptor has localized Ala380^2 to the receptor's TMH7, close to the phospholipid bilayer headgroup/water interface *in situ* (*17*, *33*). We conducted ^{2}H NMR studies of hCB$_1$(T377-E416) site-specifically CD$_3$-labeled at Ala380 with the peptide either mechanically aligned normal to the bilayer and parallel to the static magnetic field or unoriented. In the fully hydrated, aligned samples, the quadrupolar splitting of Ala380 was 31.0 ± 0.1 kHz in DMPC bilayers (Figure 1A) and 32.5 ± 0.1 kHz in POPC bilayers (Figure 1B) (means ± variance, n = 3 trials), a mean difference well beyond experimental error (±0.1). For unoriented samples, the rotational motion about the C_α−C_β Ala bond axis ideally would yield a single Pake doublet characterized by jumps among three sites with a quadrupolar splitting of about 40 kHz. In accord with this expectation, the ^{2}H quadrupole splitting of Ala380 in unoriented, partially hydrated samples of hCB$_1$(T377-E416) in POPC bilayers is indeed 40 kHz (Figure 1C), suggestive of a peptide with restricted side-chain mobility. The resolved Pake doublets of the oriented samples clearly show that the peptide is well aligned in both POPC and DMPC bilayers as compared to the powder spectrum and also indicate that the peptide is embedded within the phospholipid matrix (Figure 1A−C). The smaller quadrupolar splitting in the hydrated, aligned hCB$_1$(T377-E416) sample is most likely due to increased Ala380 mobility as compared to that in the powder sample. For the TMH7/H8 peptide in the DMPC bilayer, along with the 31 kHz Pake doublet, we also observed peaks from the evidencing quadrupolar splittings of 10.3 and 14.1 kHz not present when the peptide was in a POPC bilayer. We attribute these inner Pake doublets to conformational heterogeneity of the hCB$_1$(T377-E416) peptide in the DMPC membrane environment.

Although the methyl group's mobility and the three chemically equivalent deuterons of the CD$_3$-Ala label afford a high signal intensity relative to solid-state ^{15}N NMR (*34*−*36*), NMR of site-specifically ^{15}N-Ala-labeled peptides can provide information on their backbone secondary structure and topology (*23*). For this purpose, we studied by solid-state NMR mechanically aligned, ^{15}N-Ala380-labeled hCB$_1$(T377-E416). The spectrum of the ^{15}N-labeled TMH7/H8 CB$_1$-receptor peptide when aligned in a DMPC bilayer exhibits a rather broad resonance with a chemical shift at 180 ppm (Figure 1D). The spectrum in Figure 1E is that of an aligned hCB$_1$(T377-E416) sample in a POPC bilayer. The relatively sharp resonance peak at 200 ppm is due to the ^{15}N-labeled Ala380 residue. The NMR spectrum in Figure 1F was obtained from an unoriented, ^{15}N-Ala380-labeled TMH7/H8 peptide in a POPC bilayer. The spectrum of unoriented hCB$_1$(T377-E416) spans 215−70 ppm, indicating that, in the NMR time scale, the peptide backbone within the membrane is quite rigid. In either a POPC (Figure 1F) or DMPC (not shown) membrane environment, the ^{15}N powder pattern spectra of hCB$_1$(T377-E416) displayed the same widths/chemical shift spans, implying that backbone mobility is identical on the NMR time scale in both environments. The validity of this conclusion is supported by the identical peptide concentrations, molar peptide/lipid ratios, and number of transients for both the DMPC and POPC samples analyzed. The carbonyl-to-carbonyl thickness of the membrane mimetics differed, being about 23 Å for the DMPC bilayer and 27 Å for the POPC bilayer, with a further 10 Å to be added to these figures to account for the choline headgroups (*37*). The effective hydrophobic peptide length of the hCB1(T377-E416) transmembrane region (i.e., T377-L399) (*18*, *19*, *21*) was estimated to be 34.5 Å, assuming a perfect α-helical structure (*38*).

With respect to CB$_1$-receptor TMH7/H8 topology, the ^{15}N-Ala380 resonance peaks of the peptide in either the POPC or DMPC bilayer correspond to the 0° edge of the powder pattern (downfield). This indicates that the ^{15}N-labeled peptide backbone is parallel to the bilayer normal and is embedded within the bilayer. The difference in chemical shift between POPC and DMPC bilayers reflects a change in peptide orientation from one phospholipid environment to the other, a potential response suggested by our previous molecular dynamics simulation and modeling data (*38*). The envelope of spectral overlap in the narrower DMPC bilayer implies a greater peptide conformational heterogeneity than in the POPC bilayer, as was also indicated by the ^{2}H NMR data presented above. The same ^{2}H Pake quadrupolar splittings and ^{15}N chemical shifts as shown in Figure 1 for the mechanically aligned samples were obtained at temperatures up to 50 °C (323 K) (data not shown), indicating that the peptide retains its transmembrane alignment at higher temperatures.

SDSL/EPR Studies of hCB$_1$(T377-E416) in Membrane Phospholipid Bilayers. In conjunction with SDSL, EPR spectroscopy has emerged as a sensitive method to probe local protein dynamics and conformation (*39*, *40*). Both overall molecular tumbling and local motion of a nitroxide spin label affect EPR line shape (*41*). Detailed information about the local dynamics of spin-labeled peptides may be obtained by least-squares analysis of the EPR spectral line shape of singly labeled peptides (*42*). We investigated the local conformational dynamics of the TMH7/H8 peptide within discrete membrane-mimetic phospholipid bilayers by applying SDSL/EPR to hCB$_1$(T377-E416) spin-labeled at a cysteine residue (Cys382) localized by homology modeling

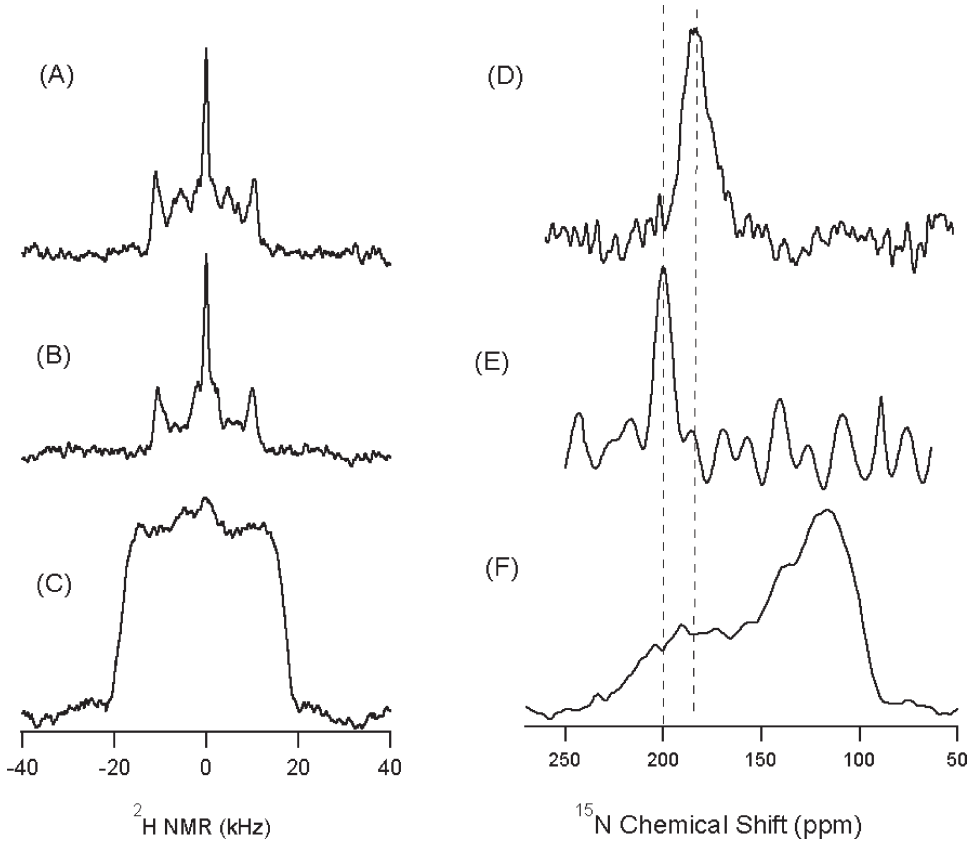

FIGURE 1: One-dimensional solid-state NMR spectra of hCB_1(T377-E416) site-specifically ^{2}H- or ^{15}N-labeled at Ala380 in POPC or DMPC bilayers. The spectra displayed were collected at 308 K. Chemical shift tensor of (A) oriented hCB_1(T377-E416) ^{2}H-labeled at Ala380 in a DMPC bilayer, (B) oriented hCB_1(T377-E416) ^{2}H-labeled at Ala380 in a POPC bilayer, (C) unoriented hCB_1(T377-E416) ^{2}H-labeled at Ala380 in a POPC bilayer, (D) oriented hCB_1(T377-E416) ^{15}N-labeled at Ala380 in a DMPC bilayer, (E) oriented hCB_1(T377-E416) ^{15}N-labeled at Ala380 in a POPC bilayer, and (F) unoriented hCB_1(T377-E416) ^{15}N-labeled at Ala380 in a POPC bilayer.

(*11*, *15*, *18*, *19*, *21*) near the phospholipid bilayer headgroup/water interface. The nitroxide spin label utilized reacts covalently and selectively with cysteine residues by forming a stable thioether bond (Figure 2) (*43*). Figure 3 shows the EPR spectra at 308 K of the hCB_1-receptor TMH7/H8 peptide labeled at Cys382 and reconstituted in a POPC or DMPC bilayer or a TFE/H_2O mixture. The spectral line shapes observed for hCB_1(T377-E416) in either TFE/H_2O or the POPC bilayer are similar, indicating that the nitroxide spin label is experiencing similar structural environments, consistent with fast tumbling of the polypeptide and reorientation of the flexible nitroxide tether. In contrast, the nitroxide EPR spectrum of the TMH7/H8 peptide in the DMPC bilayer is markedly different, with broadening of the resonance lines and line shape features, suggestive of a nitroxide tether having comparatively less mobility when hCB_1(T377-E416) is in the DMPC rather than the POPC bilayer or in TFE/H_2O.

Nonlinear least-squares line shape analysis was used to estimate rotational diffusion parameters with respect to the nitroxide molecular frame ($R_\parallel$ and $R_\perp$), isotropic hyperfine spitting (A_{iso}), and mobility parameter (ΔH_0^{-1}) for the TMH7/H8 polypeptide reconstituted in TFE/H_2O or in a bilayer of either POPC or DMPC. Two-site fitting was chosen based on spectral features (e.g., peak asymmetry, shoulder features) suggestive of the presence of multiple components (Table 1). The rotational (and more qualitative) mobility parameters support the conclusion from the EPR spectra (above) that the nitroxide spin label experiences similar dynamic environments in TFE/H_2O and POPC bilayers; in the DMPC bilayer, the peptide's

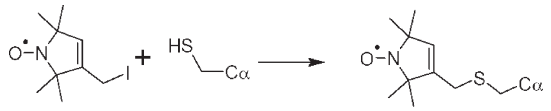

FIGURE 2: Schematic showing the reaction of nitroxide spin label [3-(iodomethyl)-2,2,5,5-tetramethyl-2,5-dihydropyrrole-1-oxyl] with a reactive cysteine [i.e., Cys382 and/or Cys386 of hCB_1(T377-E416)] to form a thioether linkage with a target peptide.

mobility is considerably less. In the TFE/H_2O mixture, the two sites have equivalent A_{iso}, as expected from the single hydrophilic phase, whereas the TMH7/H8 peptide in either a POPC or DMPC bilayer evidences two phases with marked differences between the two phospholipid environments. Parameters calculated for spin-labeled hCB_1(T377-E416) in the TFE/H_2O mixture also support the conclusion that the nitroxide is experiencing a low-viscosity hydrophilic solvent, in contrast to the peptide in a POPC bilayer, where it experiences both hydrophilic and hydrophobic environments. The hydrophilic environment likely reflects the proximity of the nitroxide spin label to the phospholipid headgroup/water interface. Conversely, the smaller A_{iso} values derived from the DMPC sample imply that, in this spectral component, the nitroxide is embedded within the phospholipid bilayer, a disposition restricting both peptide backbone dynamics and spin label rotameric freedom.

The effect of temperature on the dynamics of the nitroxide spin label at position Cys382 of hCB_1(T377-E416) in membrane-mimetic phospholipid bilayers was next examined. The EPR spectrum of the TMH7/H8 peptide reconstituted in POPC bilayers shows two temperature-dependent components in the 318−343 K range which

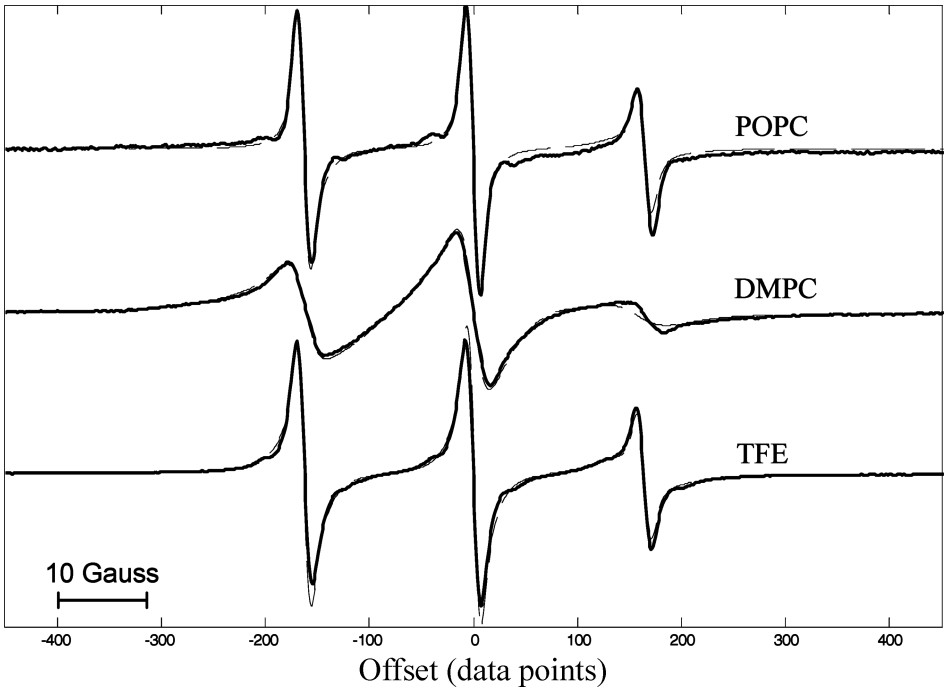

FIGURE 3: EPR spectra at 308 K of spin-labeled hCB_1(T377-E416) reconstituted in a POPC or DMPC bilayer or in TFE/H_2O. Dashed lines show the results of least-squares fitting based on the parameters in Table 1.

Table 1: Summary of Rotational Diffusion Parameters, Isotropic Hyperfine Splitting, Percent Contribution, and Mobility Parameter for hCB_1(T377-E416) in Various Environments[a]

	POPC		TFE/H_2O mixture		DMPC	
parameter	site 1	site 2	site 1	site 2	site 1	site 2
$R_{\|\|}$ [log (s^{-1})]	9.13	8.25	9.13	8.19	8.0	7.5
$R_{\perp}$ [log (s^{-1})]	8.88	8.11	8.98	8.12	8.0	7.7
A_{iso} (MHz)	45.1	43.0	45.10	45.1	43.7	43.0
%	74	26	15	85	34	66
ΔH_0^{-1} (G)	0.73		0.68		0.3	

[a] Summary of parallel ($R_{||}$) and perpendicular ($R_{\perp}$) rotational correlation times [expressed as log (s^{-1})], isotropic hyperfine spitting (A_{iso} in MHz), the percent contribution, and mobility parameter [ΔH_0^{-1} in gauss (G)] calculated from nonlinear least-squares fits of spin-labeled hCB_1(T377-E416) in a POPC bilayer, TFE/H_2O, or a DMPC bilayer at 308 K. Fixed parameters in the fits include g-factor (g_x, g_y, g_z) = (2.0085, 2.0056, 2.0020) and heterogeneous Gaussian line width of 1 G.

are particularly prominent at higher temperatures (Figure 4). We used a two-site fitting to estimate A_{iso} and extract the relative contribution of each component to the spectral intensity (*42*). As summarized in Table 2, the results confirm the presence of a hydrophilic phase with an A_{iso} of 45.1 MHz ("site 1") and a hydrophobic phase with an A_{iso} of 43.0 MHz ("site 2"). These data suggest that the local environment of the nitroxide spin label in the hCB_1-receptor TMH7/H8 peptide is distributed between the phospholipid bilayer headgroup/water interface and the hydrophobic POPC lipid core. At lower temperatures, the hydrophilic phase component accounts for 74% of the spectral intensity. As the temperature increases, the fractional hydrophobic component increases, to 85% of the spectral intensity at 343 K. This temperature-dependent behavior is reversible upon sample cooling (data not shown). The EPR spectrum of hCB_1(T377-E416) in TFE/H_2O evidences minor temperature-induced changes attributable to increased peptide mobility and lower solvent viscosity at higher temperatures (Figure 5A). By comparison, reconstitution of the TMH7/H8 peptide in DMPC bilayers significantly increases spin label mobility at higher temperatures (Figure 5B).

The equilibrium constant for the temperature-dependent hydrophilic/hydrophobic partitioning of the hCB_1(T377-E416) TMH7/H8 peptide in POPC bilayers was estimated from the relative populations calculated from the least-squares fits. Figure 6 presents a van't Hoff plot from which enthalpy (ΔH = +62.7 kJ/mol) and entropy ($T\Delta S$ = +60 kJ/mol) changes were derived for the hydrophobic-to-hydrophilic environment transition. The positive signs for ΔH and ΔS are consistent with a thermally driven immersion of the polar spin label into the hydrophobic membrane interior, where the value of ΔH reflects the energy required to localize the polar probe in the hydrophobic environment (*44*, *45*).

Spin−spin dipolar interaction in peptides labeled with two spin probes allows accurate extraction from the continuous wave EPR spectrum of interspin separations in the 5−20 Å range (*46*). Spectral reconstruction offers a means to evaluate the broadening from dipolar interaction as well as the percentage of noninteracting component caused by incomplete labeling or misfolding of the labeled peptide, leading to interspin separations beyond the 20 Å detection limit (*47*). hCB_1(T377-E416) contains two unique cysteine residues, Cys382 and Cys386, positioned within a complete turn of i to i + 4 in TMH7 (*16*, *22*, *33*). Thus, SDSL/EPR analysis of this peptide double-labeled at these cysteines would allow determination of dipolar interactions between i and i + 4, from which the distance between the two spin labels could be estimated using a dipolar broadening deconvolution method (*47*). Figure 7 shows the rigid limit EPR spectra for the doubly labeled CB_1-receptor TMH7/H8 peptide in each phospholipid environment studied. hCB_1(T377-E416) reconstituted in either TFE/H_2O solution or a POPC bilayer exhibits a significantly greater fraction of coupled spins than the peptide reconstituted in a DMPC bilayer (Table 3). Since all samples examined were prepared in parallel from the same labeled TMH7/H8 peptide

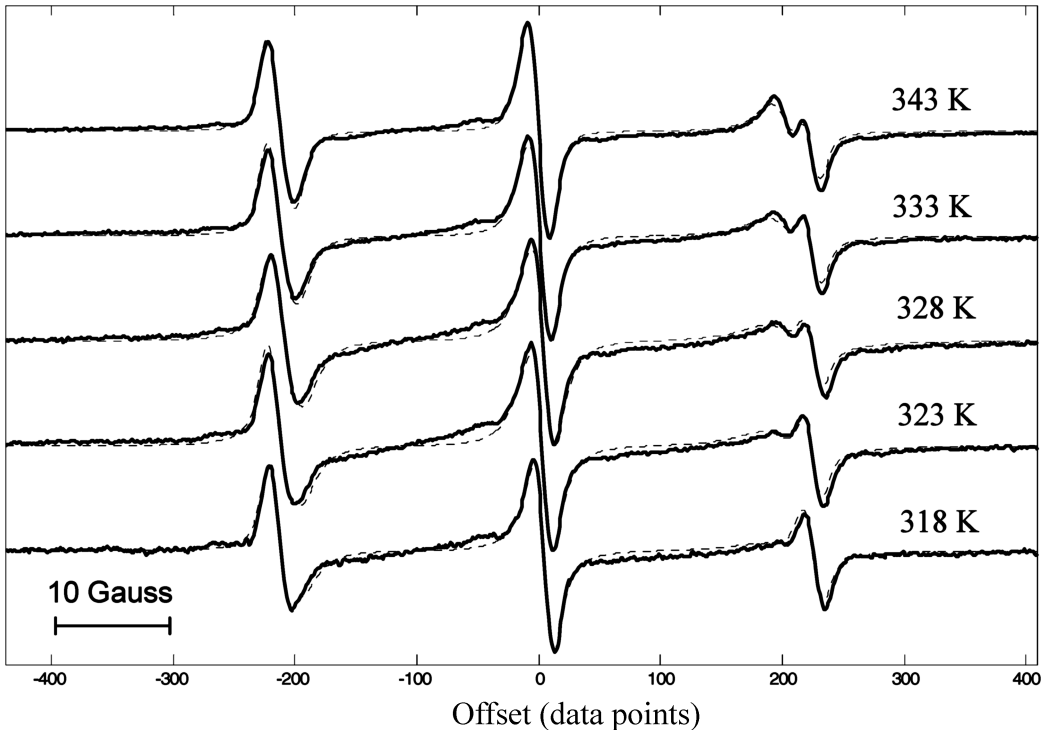

FIGURE 4: EPR spectra of spin-labeled hCB_1(T377-E416) reconstituted in a POPC bilayer at temperatures from 318 to 343 K. Dashed lines show the results of two-site least-squares fitting. For the hydrophilic site, A_{iso} = 45.1 MHz; for the hydrophobic site, A_{iso} = 43.0 MHz. Fixed parameters in the fits include *g*-factor (g_x, g_y, g_z) = (2.0085, 2.0056, 2.0020) and heterogeneous Gaussian line width of 1 G.

Table 2: Fitting Parameters for Singly Labeled hCB_1(T377-E416) Reconstituted in POPC Bilayers at Different Temperatures[a]

	log $R_{\|}$		log $R_{\perp}$		
temp (K)	site 1	site 2	site 1	site 2	population site 1 (%)
308	9.13	8.25	8.88	8.11	74
323	9.25	8.25	8.64	8.5	38
328	9.33	8.28	8.55	8.75	35
333	9.5	8.35	8.57	8.89	21
343	9.45	8.53	8.6	8.88	15

[a] Fitting parameters derived from two-site least-squares fits of singly labeled hCB_1(T377-E416) reconstituted in a POPC bilayer at different temperatures. "Site 1" represents the hydrophilic component with a fixed A_{iso} of 45.1 MHz and (g_x, g_y, g_z) = (2.0085, 2.0056, 2.0020). "Site 2" describes the hydrophobic component with a fixed A_{iso} of 43.0 MHz and (g_x, g_y, g_z) = (2.0085, 2.0056, 2.0020). $R_{\|}$ and $R_{\perp}$ correspond to the parallel and perpendicular rotational correlation times, respectively, and are expressed in units of log (s^{-1}).

stock, the drastic reduction in dipolar coupling in the DMPC sample most likely reflects a conformational heterogeneity of the peptide in DMPC that brings the paramagnetic centers out of the 20 Å range observable by the dipolar broadening technique.

DISCUSSION

The membrane phospholipid bilayer has been shown to influence rhodopsin's overall helical content and the orientation of its TMHs (*4*, *48*). However, the many distinguishing features of CB receptors preclude general extrapolation of rhodopsin TMH properties and dynamics to them and support direct experimental analysis of CB-receptor structure and conformational properties (*15*, *16*). We have used the well-validated experimental approaches of solid-state NMR and SDSL/EPR to define the conformational responsiveness of hCB_1(T377-E416) to its membrane phospholipid environment. Representing the hCB_1 receptor segment consisting of TMH7 and its intracellular α-helical extension (H8), the hCB_1(T377-E416) peptide is a domain strongly linked to this GPCR's activity and stability (*16*, *19*, *21*).

Differences observed in the ^2H and ^{15}N NMR spectra of hCB_1(T377-E416) with change of phospholipid (i.e., POPC or DMPC) bilayer matrix suggest that membrane thickness dynamically affects hCB_1(T377-E416) structural ordering, the TMH7/H8 peptide displaying greater disorder in the thinner DMPC bilayer than in the thicker POPC bilayer. As evidenced by our double-label EPR data, the high degree of coupling between spin labels located at *i* and *i* + 4 is strongly indicative of an α-helical structure for hCB_1(T377-E416) in TFE/H_2O or in a POPC bilayer, whereas the peptide undergoes a conformational adjustment in the thinner DMPC bilayer that causes the interspin distances to exceed the 20 Å detection limit of the dipolar interaction technique. The conformational adjustment is indicative of the sensitivity and adaptability of a critical helical region of the hCB_1 receptor to at least one physical property of its phospholipid matrix. Within TMH7, Pro394 is found in the highly concerved GPCR $NP(X)_nY$ motif considered important to GPCR conformational flexibility (*1*, *2*). Molecular dynamics simulations have indeed suggested that a decrease in phospholipid chain length (i.e., a thinner membrane bilayer) may induce a kink at Pro394 in TMH7 to avoid energetically unfavorable hydrophobic mismatch (*38*). Other factors including distinctive peptide−lipid interactions, decreased wobbling of the side-chain Ala380, and/or a change in peptide tilt might have contributed to the hCB_1(T377-E416) structural differences suggested by the ^2H and ^{15}N NMR spectra when the peptide is in the POPC versus the DMPC environment.

In order to characterize further the structural changes in hCB_1(T377-E416) in response to its associated phospholipid

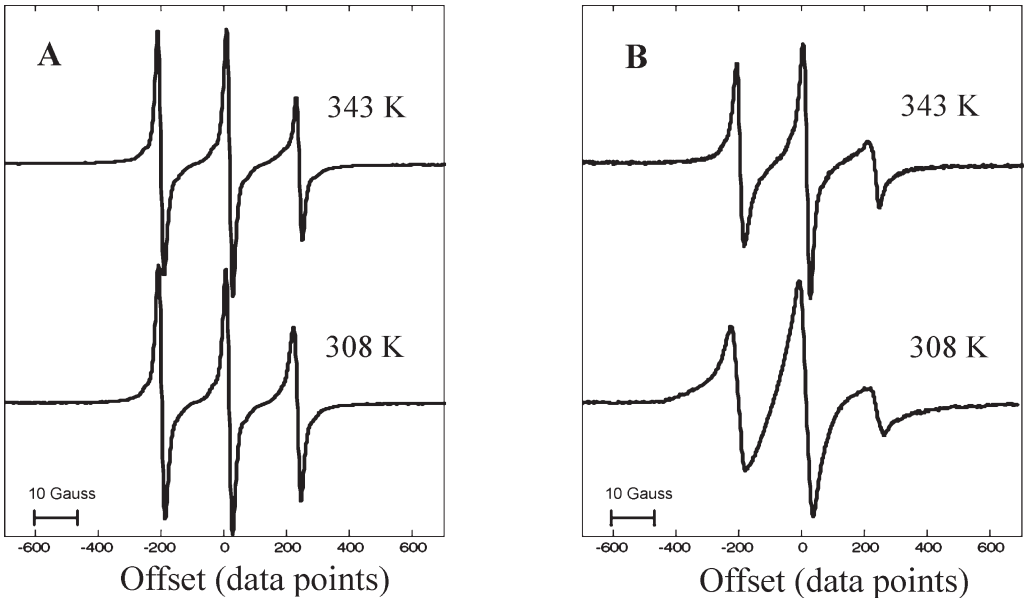

FIGURE 5: EPR spectra of hCB_1(T377-E416) singly labeled at Cys382 and reconstituted into (A) TFE/H_2O or (B) a DMPC bilayer at 308 and 343 K.

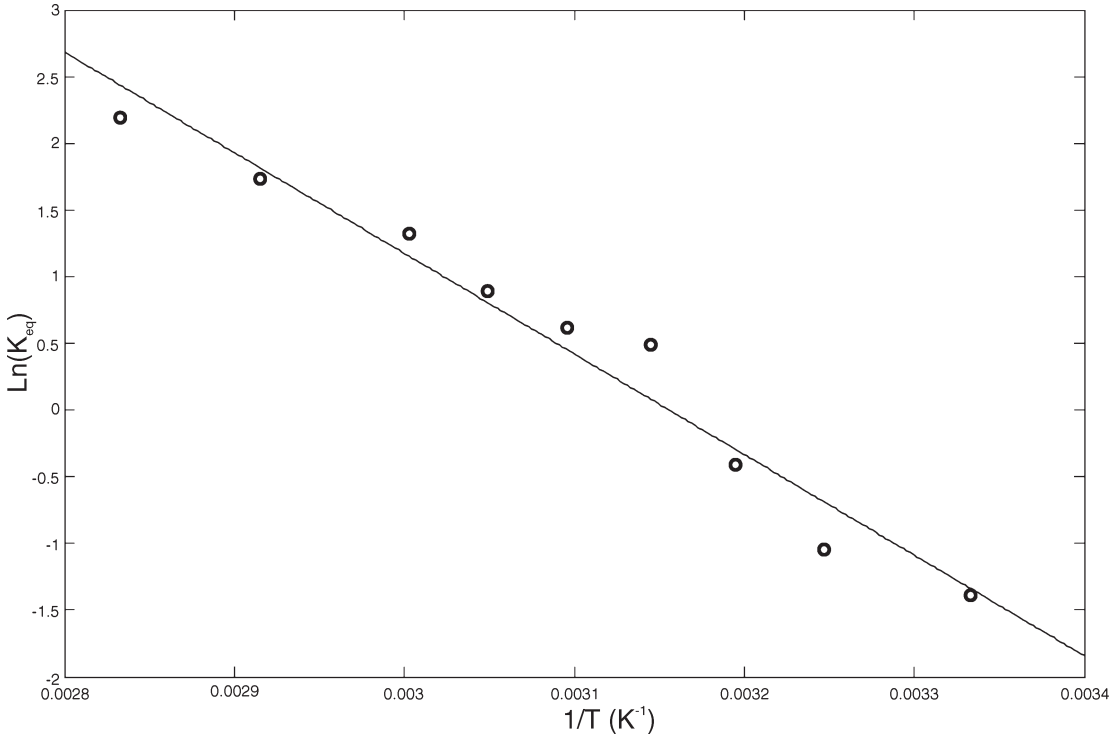

FIGURE 6: Van't Hoff plot derived from relative populations of hydrophobic/hydrophilic hCB_1(T377-E416) components as a function of temperature. The equilibrium constant K at temperature T was computed from the ratio of relative populations of hydrophobic to hydrophilic components derived from the fits. The best fit line [$\ln(K) = 7542/T + 23.8$] provides the estimates $\Delta H = +62.7$ kJ/mol and $T\Delta S = +60$ kJ/mol for the transition from hydrophobic to hydrophilic environment.

bilayer that were suggested by our NMR data, we applied the more sensitive, complementary SDSL/EPR technique. EPR spectra of hCB_1(T377-E416) spin-labeled at Cys382 are indicative of marked differences in the local dynamics of the TMH7/H8 peptide when reconstituted in TFE/H_2O solvent or either POPC or DMPC bilayers. hCB_1(T377-E416) evidences fast motional spectral line shapes in TFE/H_2O and POPC which contrast with the more complex slow motional spectrum observed for the peptide in DMPC. EPR analysis of hCB_1(T377-E416) reconstituted in a POPC bilayer over the temperature range 308−343 K revealed the presence of two spectral components attributable to a hydrophilic phase predominant at lower temperatures and a hydrophobic phase more pronounced at higher temperatures. Partitioning between hydrophobic and hydrophilic environments suggests that the nitroxide spin label resides near the phospholipid bilayer headgroup/water interface. As the temperature is increased, the TMH7/H8 peptide appears to undergo conformational change that positions the spin label in a more hydrophobic environment. This interpretation is supported by the positive ΔH and ΔS values extracted from van't Hoff analysis of the relative

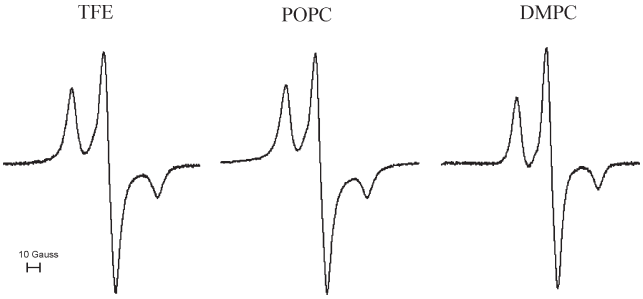

FIGURE 7: Rigid limit spectra of doubly labeled hCB_1(T377-E416) in TFE/H_2O or in a bilayer composed of either POPC or DMPC. All spectra were signal averaged for 30 scans.

Table 3: Results from Dipolar Deconvolution for the Three Peptide Environments Examined[a]

environment	average distance (Å)	distribution (Å)	% coupling
TFE/H_2O	10.6 ± 1.5	8 ± 3.5	50 ± 1.7
POPC	16.8 ± 0.5	6.2 ± 3.5	60.3 ± 3.5
DMPC	11.6 ± 2	6.2 ± 5	14.3 ± 1

[a] The error was estimated using a 90% tolerance around the best χ^2 value.

populations. In contrast, the peptide's nitroxide reporter shows a distinct orientation and dynamic in a DMPC bilayer and does not undergo the same temperature-dependent partitioning that it did in the POPC lipid environment. Analogous EPR experiments have demonstrated that the influence of temperature on the conformational stability of various peptides associated with phospholipid membranes varies widely, from slight (*44*) to significant (*45*).

Figure 8 presents a conceptual schematic of hCB_1(T377-E416) derived from a previously published molecular dynamics simulation of the peptide in POPC/DMPC bilayers (*38*) into which the nitroxide spin label at Cys382 has now been placed. In the prior work, Cys382 was placed close to the phospholipid headgroup/water interface, and the tilt angle of TMH7 was determined to be 13 ± 3° in the POPC bilayer and 28 ± 5° in the DMPC bilayer. The angle between TMH7 and H8 was determined to be 89 ± 5° in the POPC bilayer and 119 ± 7° in the DMPC bilayer, the increased tilt proposed to reflect a Pro394 kink in TMH7 when the peptide resides in the thinner DMPC bilayer. The measured 16.8 Å interspin distance between Cys382 and Cys386 (i to i + 4) when the hCB_1 peptide is in a POPC bilayer is indicative of an extended helix, which justifies positioning the nitroxide reporter group close to the headgroup/water interface. This interspin distance is somewhat greater than that estimated for an ideal α-helical structure in solution (*49*). The difference may reflect the orientation of the spin label tether in the membrane as compared to the tether orientation in solution, the latter representing the model system from which the estimate was derived. Furthermore, the comparator interspin-distance estimates on doubly labeled model peptides (*49*) employed as spin label methanethiosulfonate, which may become ordered on the protein surface as a result of interactions between the δ-sulfur and the protein's backbone obviated by our use of the 3-(iodomethyl)-2,2,5,5-tetramethyl-2,5-dihydropyrrole-1-oxyl spin label (*41*). As the temperature is elevated, the probe more frequently samples the hydrophobic environment due to increased peptide motion and membrane dynamics. In DMPC, the majority of the interspin distances observed for hCB_1(T377-E416) are outside the range of the

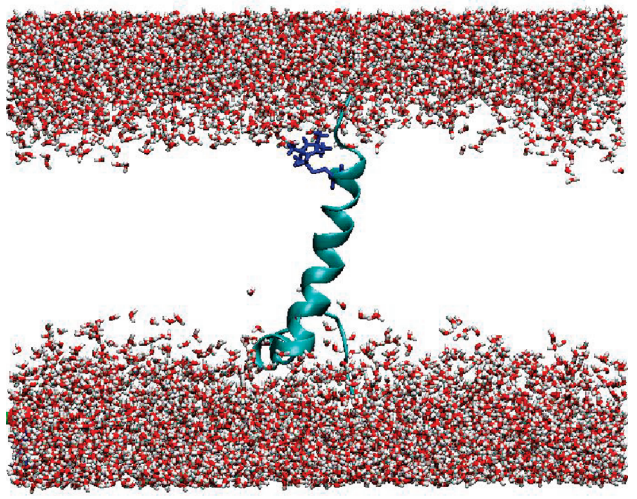

FIGURE 8: Schematic representation of the intramembrane portion of hCB_1(T377-E416) in a POPC bilayer with the nitroxide spin label at Cys382 depicted in blue. The depiction highlights the proximity of the nitroxide reporter group to the phospholipid headgroup/water interface.

dipolar-broadening technique applied here. However, the measured distance of 11.6 Å, which corresponds to only 14% of peptide population, places the spin probe well within the hydrophobic bilayer. The apparent conformational heterogeneity of hCB_1(T377-E416) in DMPC contrasts with the situation when the peptide is in POPC, where more than 60% of the peptide population produces dipolar coupling. We take this as further evidence that the phospholipid bilayer directly affects the conformation of the hCB_1(T377-E416) TMH, which in turn appears sensitive and adaptable to its membrane environment. Diverse physical and biochemical characteristics of phospholipid membranes can influence transmembrane protein (including GPCR) structure and function (*50*). Accordingly, factors other than bilayer thickness/hydrophobic matching may have played a part in the hCB_1(T377-E416) structural differences noted between DMPC and POPC, perhaps interactively. For example, the monounsaturated nature of the oleoyl moiety of POPC vs the fully saturated DMPC fatty-acyl groups means that bilayers composed of these lipids have intrinsically distinct molecular ordering, expansiveness, and fluidity properties that could affect transmembrane protein conformation, lateral diffusion/mobility, interaction, and distribution (*50*, *51*). Although the occurrence of peptide aggregation on the DMPC bilayer surface cannot be excluded as contributing to the relatively lower coupling in that membrane environment (Table 3), the decrease in dipolar interaction observed in DMPC suggests that peptide aggregation is not a significant contributor to the hCB_1(T377-E416) structural dynamics documented.

Given the importance of its C-terminal component to the activity and stability of the hCB_1 receptor and other GPCRs (*2*, *16*, *19*, *21*, *52*), the results presented have implications for the biological function of the CB_1 receptor and, perhaps, GPCRs in general. Conserved proline residues have been implicated in the mobility and signal-transducing capability of various GPCR TMHs (*1*, *2*). Consequently, it may be hypothesized that a kink at Pro394 in the $NP(X)_nY$ microdomain of TMH7 (*38*), which is highly conserved across class A GPCRs (*1*, *2*), could be crucial to the conformational plasticity of the C-terminal segment of the hCB_1 receptor we have documented. In this manner, Pro394 may be a component of a sensitive response mechanism that allows the

CB_1 receptor to adjust its conformation to varied hydrophobic membrane domains during its internalization, intracellular transit, and activation (*5*). Our observations support the proposition that peptide conformational responses to membrane bilayer properties are a hallmark of GPCRs important to their activation and consequent downstream signaling (*6*). The potential of mutual structural accommodation between GPCRs (including the CB_1 receptor) and their membrane environment to affect GPCR transmission has implications for GPCR-targeted drug discovery (*1*, *6*).

REFERENCES

1. Langerström, M. C., and Schöth, H. B. (2008) Structural diversity of G protein-coupled receptors and significance for drug discovery. *Nat. Rev. Drug Discovery 7*, 339–357.
2. Kobilka, B. (2007) G protein coupled receptor structure and activation. *Biochim. Biophys. Acta 1768*, 794–807.
3. Urizar, E., Claeysen, S., Depuí, X., Govaerts, C., Costagliola, S., Vassart, G., and Pardo, L. (2005) An activation switch in the rhodopsin family of G protein-coupled receptors: the thyrotropin receptor. *J. Biol. Chem. 280*, 17135–17141.
4. Altenbach, C., Kusnetzow, A. K., Ernst, O. P., Hofmann, K. P., and Hubbell, W. L. (2008) High-resolution distance mapping in rhodopsin reveals the pattern of helix movement due to activation. *Proc. Natl. Acad. Sci. U.S.A. 105*, 7439–7444.
5. Leterrier, C., Bonnard, D., Carrel, D., Rossier, J., and Lenkei, Z. (2004) Constitutive endocytic cycle of the CB1 cannabinoid receptor. *J. Biol. Chem. 279*, 36013–36021.
6. Gawrisch, K., and Soubias, O. (2008) Structure and dynamics of polyunsaturated hydrocarbon chains in lipid bilayers—significance for GPCR function. *Chem. Phys. Lipids 153*, 64–75.
7. Lee, A. G. (2004) How lipids affect the activities of integral membrane proteins. *Biochim. Biophys. Acta 1666*, 62–87.
8. Vemuri, V. K., Janero, D. R., and Makriynannis, A. (2008) Pharmacotherapeutic targeting of the endocannabinoid system: drugs for obesity and the metabolic syndrome. *Physiol. Behav. 93*, 671–686.
9. Mackie, K. (2008) Cannabinoid receptors: where they are and what they do. *J. Neuroendocrinol. 20*(Suppl. 1), 10–14.
10. Lu, D., Guo, J., Duclos, R. I.Jr., Bowman, A. L., and Makriyannis, A. (2008) Boronyl- and isoboronyl-Δ^8-tetrahydrocannabinols: a novel class of cannabinergic ligands. *J. Med. Chem. 51*, 6393–6399.
11. Pei, Y., Mercier, R. W., Anday, J. K., Thakur, G. A., Zvonok, A. M., Hurst, D., Reggio, P. H., Janero, D. R., and Makriyannis, A. (2008) Ligand-binding architecture of human CB2 cannabinoid receptor: evidence for receptor subtype-specific binding motif and modeling GPCR activation. *Chem. Biol. 15*, 1207–1219.
12. Pertwee, R. G. (2008) The diverse CB1 and CB2 receptor pharmacology of three plant cannabinoids: Δ^9-tetrahydrocannabinol, cannabidiol and Δ^9-tetrahydrocannabivarin. *Br. J. Pharmacol. 153*, 199–215.
13. Janero, D. R., and Makriyannis, A. (2009) Cannabinoid-receptor antagonists: pharmacological opportunities, clinical experience, and translational prognosis. *Expert Opin. Emerging Drugs 14*, 43–65.
14. Janero, D. R., and Makriyannis, A. (2007) Targeted modulators of the endogenous cannabinoid system: future medications to treat addiction disorders and obesity. *Curr. Psychiatry Rep. 9*, 365–373.
15. Tuccinardi, T., Ferrarini, P. L., Manera, C., Ortore, G., Saccomanni, G., and Martinelli, A. (2008) Cannabinoid CB2/CB1 selectivity. Receptor modeling and automated docking analysis. *J. Med. Chem. 49*, 984–994.
16. Reggio, P. H. (2005) Cannabinoid receptors and their ligands: ligand-ligand and ligand-receptor modeling approaches. *Handb. Exp. Pharmacol. 168*, 247–281.
17. Kapur, A., Hurst, D. P., Fleischer, D., Whitnell, R., Thakur, G. A., Makriyannis, A., Reggio, P. H., and Abood, M. E. (2007) Mutation studies of Ser7.39 and Ser2.60 in the human CB1 cannabinoid receptor: evidence for a serine-induced bend in CB1 transmembrane helix 7. *Mol. Pharmacol. 71*, 1512–1524.
18. Whitnell, R. M., Hurst, D. P., Reggio, P. H., and Guarnieri, F. (2008) Conformational memories with variable bond angles. *J. Comput. Chem. 29*, 741–752.
19. Anavi-Goffer, S., Fleischer, D., Hurst, D. P., Lynch, D. L., Barnett-Norris, J., Shi, S., Lewis, D. L., Mukhopadhyay, S., Howlett, A. C., Reggio, P. H., and Abood, M. E. (2008) Helix 8 leu in the CB_1 cannabinoid receptor contributes to selective signal transduction mechanisms. *J. Biol. Chem. 282*, 25100–25113.
20. Ballesteros, J. A., and Weinstein, H. (1995) Integrated methods for the construction of three dimensional models and computational probing of structure function relations in G protein-coupled receptors. *Methods Neurosci. 25*, 366–428.
21. Choi, G., Guo, J, and Makriyannis, A. (2005) The conformation of the cytoplasmic helix 8 of the CB1 cannabinoid receptor using NMR and circular dichroism. *Biochim. Biophys. Acta 1668*, 1–9.
22. Tiburu, E. K., Karp, E. S., Birrane, G., Struppe, J. O., Chu, S., Lorigan, G. A., Avraham, S., and Avraham, H. K. (2006) ^{31}P and ^{2}H relaxation studies of helix VII and the cytoplasmic helix of the human cannabinoid receptors utilizing solid-state NMR techniques. *Biochemistry 45*, 7356–7365.
23. Opella, S. J., and Stewart, P. L. (1989) Solid-state nuclear magnetic resonance structural studies of proteins. *Methods Enzymol. 179*, 242–275.
24. Makriyannis, A., Banijamali, A., Van der Schyf, C., and Jarrell, H. (1987) Interactions of cannabinoids with membranes. The role of cannabinoid stereochemistry and absolute configuration and the orientation of Δ^9-THC in the membrane bilayer. *NIDA Res. Monogr. 79*, 123–133.
25. Dave, P. C., Tiburu, E. K., Damodaran, K., and Lorigan, G. A. (2004) Investigating structural changes in the lipid bilayer upon insertion of the transmembrane domain on the membrane-bound protein phospholamban utilizing ^{31}P and ^{2}H solid-state NMR spectroscopy. *Biophys. J. 86*, 1564–1573.
26. Abu-Baker, S., Lu, J. X., Chu, S., Shetty, K. K., Gor'kov, P. L., and Lorigan, G. A. (2007) The structural topology of wild-type phospholamban in oriented lipid bilayers using ^{15}N solid-state NMR spectroscopy. *Protein Sci. 16*, 2345–2349.
27. Ketchem, R. R., Hu, W., and Cross, T. A. (1993) High-resolution conformation of gramicidin A in a lipid bilayer by solid-state NMR. *Science 261*, 1457–1460.
28. Davis, J. H., Jeffrey, K. R., Bloom, M., Valic, M. I., and Higgs, T. P. (1976) Quadrupolar echo deuteron magnetic resonance spectroscopy in ordered hydrocarbon chains. *Chem. Phys. Lett. 42*, 390–394.
29. Hallock, K. J., Lee, D. K., and Ramamoorthy, A. (2003) MSI-78, an analogue of the magainin antimicrobial peptides, disrupts lipid bilayer structure via positive curvature strain. *Biophys. J. 84*, 3052–3060.
30. Strandberg, E., Ozdirekcan, S., Rijkers, D. T. S., van der Wel, P. C. A., Koeppe, R. E.II, Liskamp, R. M. J., and Killian, J. A. (2004) Tilt angles of transmembrane model peptides in oriented and non-oriented lipid bilayers as determined by ^{2}H solid-state NMR. *Biophys. J. 86*, 37093721.
31. Whiles, J. A., Glover, K. J., Vold, R. R., and Komives, E. A. (2002) Methods for studying transmembrane peptides in bicelles: consequences of hydrophobic mismatch and peptide sequence. *J. Magn. Reson. 158*, 149–156.
32. Jones, D. H., Barber, K. R., VanDerLoo, E. W., and Grant, W. M. (1998) Epidermal growth factor receptor transmembrane domain: ^{2}H NMR implications for orientation and motion in a bilayer environment. *Biochemistry 37*, 16780–16787.
33. Kapur, A., Samaniego, P., Thakur, G. A., Makriyannis, A., and Abood, M. E. (2008) Mapping the structural requirements in the CB1 cannabinoid receptor transmembrane helix II for signal transduction. *J. Pharmacol. Exp. Ther. 325*, 341–348.
34. Opella, S. J. (1997) NMR and membrane proteins. *Nat. Struct. Biol. 4*, 845–848.
35. Porcelli, F., Buck, B., Lee, D. K., Hallock, K. J., Ramamoorthy, A., and Veglia, G. (2004) Structure and orientation of pardaxin determined by NMR experiments in model membranes. *J. Biol. Chem. 270*, 45815–45823.
36. Strandberg, E., Ozdirekcan, S., Rijkers, D. T. S., van der Wel, P. C. A., Koeppe, R. E.II, Liskamp, R. M. J., and Killian, J. A. (2004) Tilt angles of transmembrane model peptides in oriented and non-oriented lipid bilayers as determined by ^{2}H solid-state NMR. *Biophys. J. 86*, 3709–3721.
37. Cornell, B. A., and Separovic, F. (1983) Membrane thickness and acyl chain length. *Biochim. Biophys. Acta 733*, 189–193.
38. Tiburu, E. K., Bowman, A. L., Struppe, J. O., Janero, D. R., Avraham, H. K., and Makriyannis, A. (2009) Solid-state NMR and molecular dynamics characterization of cannabinoid receptor-1 (CB1) helix 7 conformational plasticity in model membranes. *Biochim. Biophys. Acta 1788*, 1159–1167.
39. Columbus, L., and Hubbell, W. L. (2002) A new spin on protein dynamics. *Trends Biochem. Sci. 27*, 288–295.
40. Inbaraj, J. J., Laryukhin, M., and Lorigan, G. A. (2007) Determining the helical tilt angle of a transmembrane helix in mechanically aligned lipid bilayers using EPR spectroscopy. *J. Am. Chem. Soc. 129*, 7710–7711.

41. Hubbell, W. L., Cafiso, D. S., and Altenbach, C. (2000) Identifying conformational changes with site-directed spin labeling. *Nat. Struct. Biol. 7*, 735–739.
42. Budil, D. E., Lee, S., Saxena, S., and Freed, J. H. (1996) Nonlinear-least-squares analysis of slow-motion EPR spectra in one and two dimensions using a modified Levenberg-Marquardt algorithm. *J. Magn. Reson., Ser. A 120*, 155–189.
43. Hurth, K. M., Nilges, M. J., Carlson, K. E., Tamrazi, A., Belford, R. L., and Katzenellenbogen, J. A. (2004) Ligand-induced changes in estrogen receptor conformation as measured by site-directed spin labeling. *Biochemistry 43*, 1891–1907.
44. Levy, Y., Jortner, J., and Becker, O. M. (2001) Solvent effects on the energy landscapes and folding kinetics of polyalanine. *Proc. Natl. Acad. Sci. U.S.A. 98*, 2188–2193.
45. Wieprechta, T., Beyermannb, M., and Seeliga, J. (2002) Thermodynamics of the coil-α helix transition of amphipathic peptides in a membrane environment: the role of vesicle curvature. *Biophys. Chem. 96*, 191–201.
46. Berliner, L. J., Eaton, S. S., and Eaton, G. R. (2003) *Biological Magnetic Resonance, Volume 19: Distance Measurements in Biological Systems by EPR*, Kluwer Academic Publishers, Dordrecht, The Netherlands.
47. Fajer, P. G. (2000) EPR of Proteins and Peptides, in *Encyclopedia of Analytical Chemistry* (Meyers, R., Ed.) pp 5725−5761, Wiley and Sons, London.
48. Soubias, O., Niu, S.-L., Mitchell, D. C., and Gawrisch, K. (2008) Lipid-rhodopsin hydrophobic mismatch alters rhodopsin helical content. *J. Am. Chem. Soc. 130*, 12465–12471.
49. Rabenstein, M. D., and Shin, Y.-K. (1995) Determination of the distance between two spin labels attached to a macromolecule. *Proc. Natl. Acad. Sci. U.S.A. 92*, 8239–8243.
50. Gawrisch, K., and Soubias, O. (2008) Structure and dynamics of polyunsaturated hydrocarbon chains in lipid bilayers—significance for GPCR function. *Chem. Phys. Lipids 153*, 64–75.
51. McIntosh, T. J., and Simon, S. A. (2006) Roles of bilayer material properties in function and distribution of membrane proteins. *Annu. Rev. Biophys. Biomol. Struct. 35*, 177–198.
52. Conner, M., Hicks, M. R., Dafforn, T., Knowles, T. J., Ludwig, C., Staddon, S., Overduin, M., Günther, U. L., Thome, J., Wheatley, M., Poyner, D. R., and Conner, A. C. (2008) Functional and biophysical analysis of the C-terminus of the CGRP-receptor, a family B GPCR. *Biochemistry 47*, 8434–8444.